Mid-infrared Detection using Black Phosphorus on Silicon Heterostructure with Avalanche Multiplication

Yen-Ju Lin[†1,2], Chien-Yu Chen[†2], Chang-Hua Liu[†1], Neil Na[†2]
[†1] Institution of Photonics Technology, National Tsing-Hua University, Hsinchu, Taiwan (R.O.C.)
[†2] Artilux Inc., Hsinchu, Taiwan (R.O.C.)
E-mail: changhua@gapp.nthu.edu.tw and neil@artiluxtech.com

ABSTRACT

An analytical method is proposed to design high-responsivity and high-speed mid-infrared (MIR) detection device with avalanche multiplication. In this work, a separated absorption, charge, and multiplication avalanche photodiode (SACM APD) using bulk black phosphorus-on-silicon (bBP-on-Si) heterostructure is calculated and simulated with punch-through near 10V and breakdown near 20V. This work reaches 1000x bandwidth improvement and high gain-bandwidth product up to 128 GHz with high responsivity as 2.75 A/W comparing with other two-dimension materials (2DM) on silicon heterostructures.

Keywords: mid-infrared, APD, 2D materials, black phosphorus

I. INTRODUCTION

Recently, two-dimension materials used for photo-detection have attracted wide attention due to the broad operation wavelengths and the flexible fabrication methods. Extending detection range to MIR allows various applications that require fast response, e.g. molecule detection in biomedical sensing, thermal imaging, environmental monitoring, and free-space communication. Previous works have reported the possibility of designing and fabricating photo-detecting devices using 2DM through various working mechanisms and material combinations [1,2]. As an example, bulk black phosphorus (bBP), a narrow bandgap 2DM, has been demonstrated to be a promising MIR photodetector by Guo [3] and Chen [4].

For MIR sensing and imaging, researchers are mainly focusing on enhancing the responsivity. However, low bandwidth is a tradeoff for acquiring a high responsivity through either thicker 2DM or photogating effect, which may limit the range of applications. In this work, we propose bBP-on-Si for implementing separate absorption, charge, and multiplication avalanche photodiode (SACM APD) [5], with bBP as the absorption layer and Si as the multiplication layer. The signal can be multiplied with avalanche gain without trading the bandwidth, which may be a viable solution for high-speed and high-responsivity MIR photodetector.

II. METHOD

Considering bBP-Si heterostructure depicted in Fig. 1(a), we use bBP as both absorption layer (AL) with thickness equals to 20 nm. Charge layer (CL) is p-doped Si with 100 nm thickness. Between AL and CL, we add an optional intrinsic Si as buffer layer (BL) for tuning high field inside

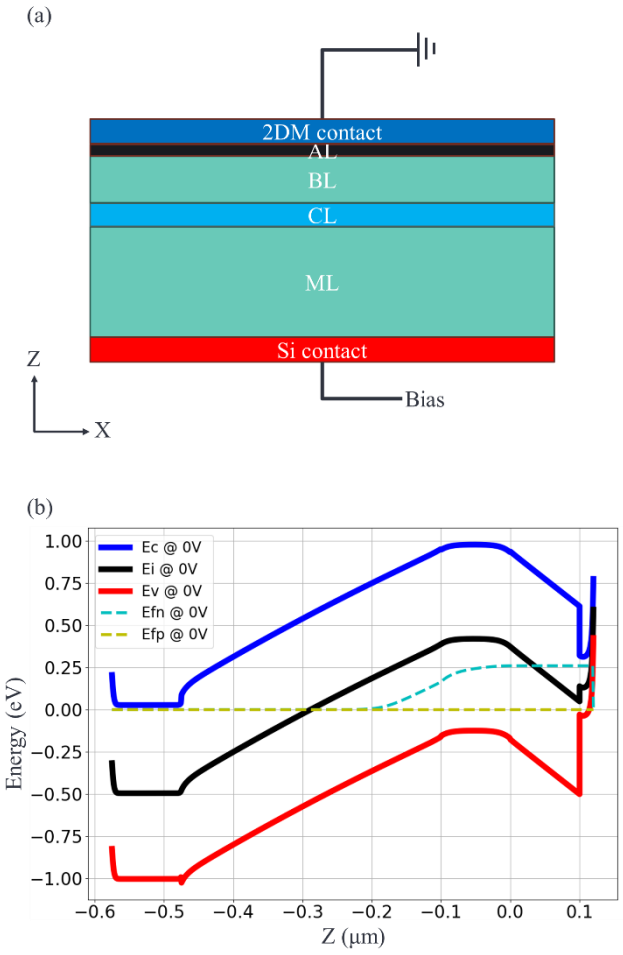

Fig 1. (a) Schematic plot of the device. (b) Band structure of the device in equilibrium using Au as contact on AL.

AL with 200 nm thickness in this case. Multiplication layer (ML) is the region where carriers been multiplicated. The thickness of this layer determines breakdown and punch-through voltage and will be discussed in Section III. Contact is doped with high n-type concentration to form Ohmic contact on Si. The electrical properties of bBP are set as follow: band structure is 0.35 eV and dc permittivity are 12.5, 10.8 and 8.3 in unit of vacuum permittivity (ε_0) along X, Y and Z axis [6]; work function is 4.3eV [7]. To simplify the breakdown model, we consider electric field along Z axis only. The device is quasi-1D along Z axis without lateral field. With the simplification, the anisotropic mobility and effective mass of bBP can be approximated to isotropic

electrical properties along Z axis. In this case, mobilities are 400 $cm^2/V \cdot s$ and 540 $cm^2/V \cdot s$ for electron and hole respectively and effective mass are 0.221 and 0.24 in unit of electron rest mass for electron and hole respectively [8].

We use finite element method (FEM) simulation with periodic boundary along X axis to derive electric field distribution. The band structure in equilibrium along Z axis as depicted in Fig. 1(b). For Si and 2DM contact, we use aluminum with work function 4.26 eV to be N contact and gold with work function 5.1 eV. Note that the contact on bBP requires large work function, i.e. larger than bBP's work function, to form P contact as shown in Fig. 2(a). Metal or other 2DM with small work function metal may form N contact for bBP-metal contact as Fig. 2(b) shows, which confirmed experimentally reported by Perello et al [7] with aluminum contacts on black phosphorus.

To characterize our device, we define three voltages: (1) unity gain (Vug), (2) punch though (Vpt) and (3) breakdown (Vbr). The unity gain voltage is the bias where impact ionization gain starts to involve. We extract the light-on current of the device with and without CL, i.e. APD and photodetector (PD) light-on current, and find the unity gain voltage where the light-on current is equal to unity gain current derived from PD. The punch through voltage is the bias where CL has been punched through, i.e. the field inside Si is purely positive from 2DM to Si contact. We scan the electric field of APD along Z axis in different bias and interpolate the voltage where electric field near top edge of CL is exactly zero.

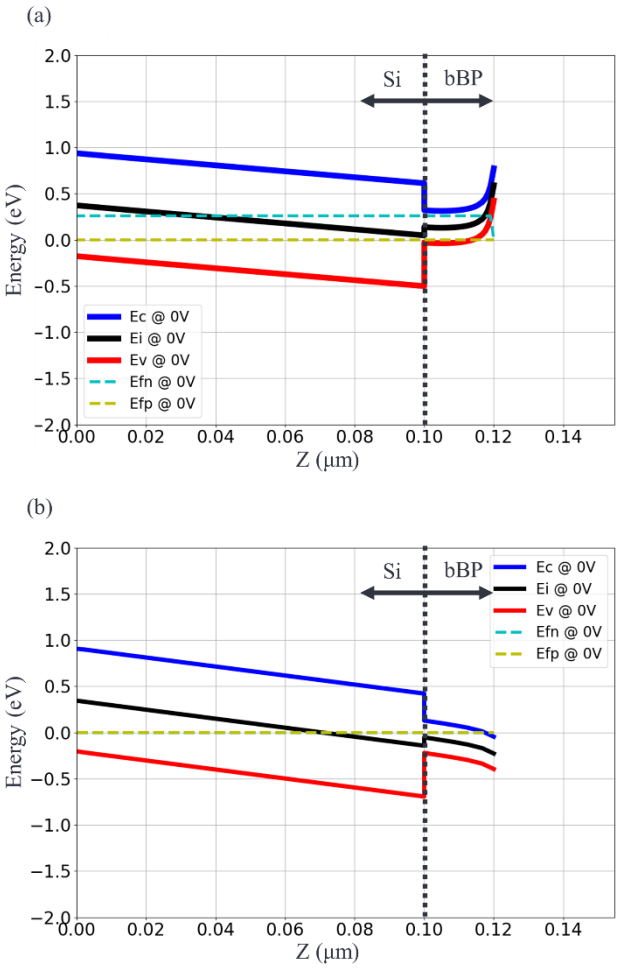

Fig 2. Zoomed in band structure in equilibrium with (a) gold as P contact and (b) aluminum as N contact on bBP.

Since the electric field varies slowly inside ML, we consider local breakdown model to evaluate breakdown voltage by the condition [9]

$$1 = \int_0^{tML} \alpha_h(x) e^{-\int_0^x (\alpha_h(x') - \alpha_e(x'))dx'} dx, \quad (1)$$

where tML is the multiplication layer thickness of the device and $\alpha_e(\alpha_h)$ are impact ionization coefficient of electron (hole) depending on electric field [10]

$$\alpha_{e/h}(x) = A_{e/h} e^{-(b_{e/h}/E(x))} dx. \quad (2)$$

where $A_{e/h}$ and $b_{e/h}$ are ionization coefficients for electron and hole respectively. To explicitly derive the gain and excess noise factor, we calculate the McIntyre formula [11]

$$M(x) = \frac{e^{-\int_x^{tML} (\alpha_e(x') - \alpha_h(x'))dx'}}{1 - \int_0^{tML} \alpha_e(x) e^{-\int_x^{tML} (\alpha_e(x') - \alpha_h(x'))dx' dx}}, \quad (3)$$

$$F(x) = k_{eff} M(x) + (2 - \frac{1}{M(x)})(1 - k_{eff}), \quad (4)$$

where k_{eff} is the effective impact ionization coefficient ratio of hole to electron.

To evaluate the performance of the device, we calculate the small signal analysis and noise equivalent power (NEP) under the bias where avalanche gain equals to 10. We apply a small voltage variation, e.g. 30 mV, onto N contact and extract small signal response. The current will be complex and frequency dependent. NEP is defined as signal power

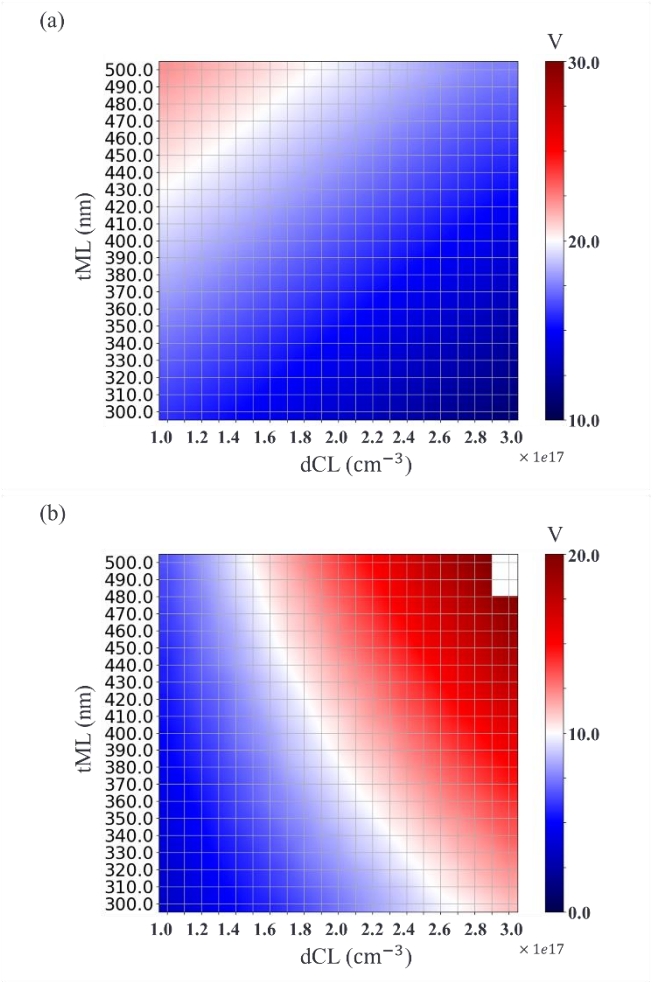

Fig 3. (a) Breakdown and (b) punch-through voltages of the SACM APD plotted as a function of ML thickness (tML) and CL concentration (dCL)

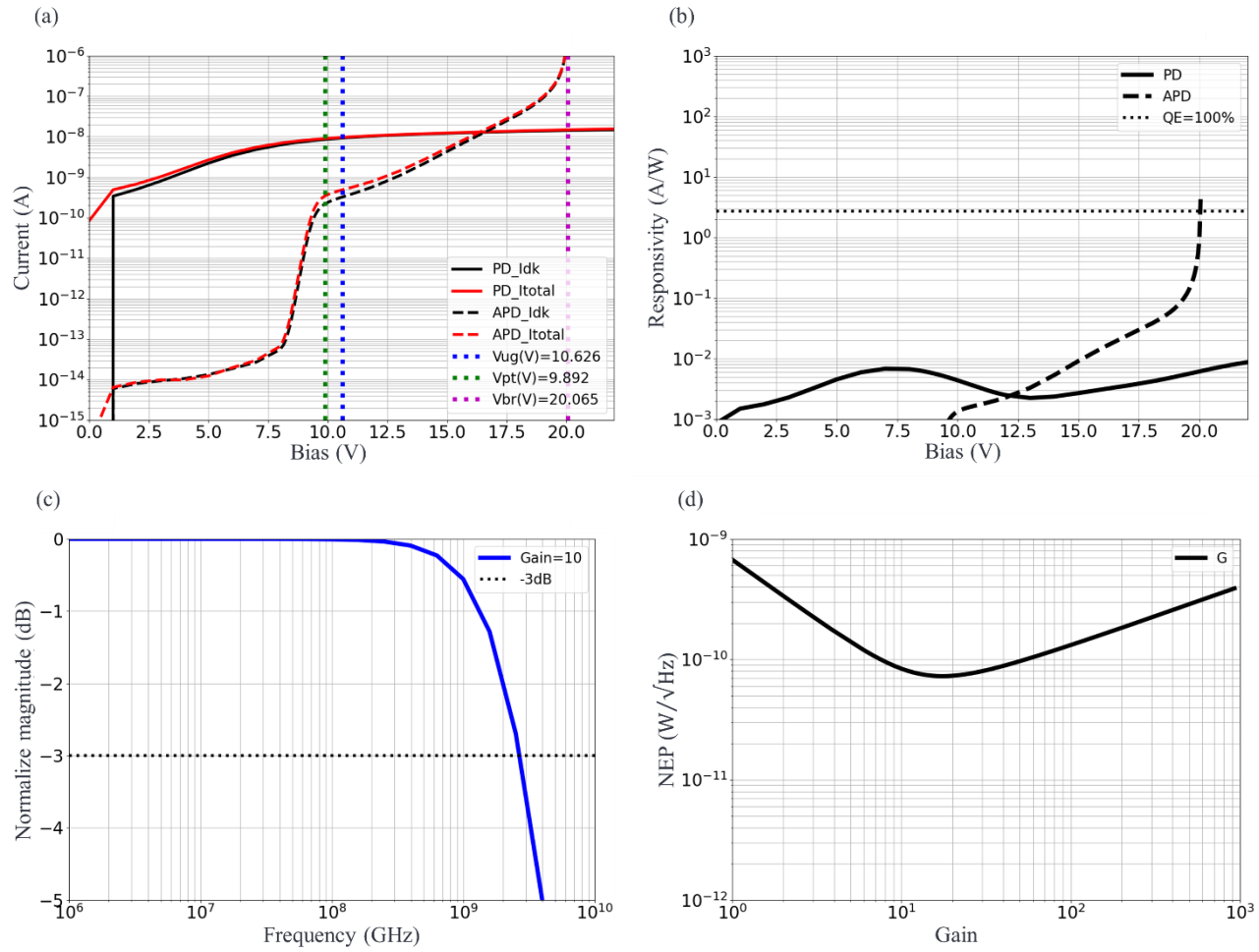

Fig 4. (a) Light-off current (black) and light-on current (red) of the reference PD (solid line) and the APD (dotted line) plotted as a function of reverse bias. (b) Responsivity of the reference PD and the APD plotted as a function of reverse bias. The "QE=100%" line indicates the theoretical maximum responsivity of the reference PD at 3400 nm wavelength. (c) Small-signal response of the APD plotted as a function of frequency given gain equal to 10. The "-3dB" line indicates the optical signal dropping to half of its low-frequency value. (d) NEP of the APD plotted as a function of gain.

where signal-to-noise ratio (SNR) equals to 1 of a 1 Hz bandwidth.

The SNR including avalanche gain and excess noise factor as follow

$$SNR = \frac{MI_{ph}}{\sqrt{I_{TIA}^2 + 2q(I_{ph}+I_{dk\_m})M^2F + 2qI_{dk\_n}}}, \quad (5)$$

$$NEP = \frac{I_{ph(SNR=1)}}{R(M=1)}, \quad (6)$$

where I_{ph}, I_{dk_m} and I_{dk_n} are photo current, multiplied dark current and non-multiplied dark current, respectively; q is elementary charge; R is the unity gain responsivity. We consider a relatively low speed transimpedance amplifier (TIA), e.g. MAX40213 from Maxim Integrated, with 1.1 pA/$\sqrt{\text{Hz}}$ for I_{TIA} in Eq. 5.

For gain device, gain-bandwidth product (GBP) is used to evaluate the bandwidth with certain gain. The GBP can be determined by Emmon's formula [12],

$$M(\omega) = \frac{M}{\sqrt{1+\omega^2 M^2 (Nk_{eff}\tau)^2}}, \quad (7)$$

where N is a number varying from 1/3 to 2 as k_{eff} varies from 1 to 0.001. τ is the transit time in the ML.

III. Result and Discussion

Through scanning the thickness of multiplication layer (ML) and the concentration of charge layer (CL), we can simulate the operating condition and the corresponding designs of ML and CL. The result design maps are shown in Fig. 3. An arbitrarily targeted APD at 20V breakdown voltage and 10V punch-through can be found with the ML thickness ~475nm and the CL concentration is 1.55e17 cm^{-3}, the resultant breakdown voltage is 20.065 V and the resultant punch-through voltage is 9.892 V. The APD current gain of this specific design can be calculated and it reaches 10 when bias at ~18.8V.

As shown by the I-V curves in Fig. 4(a), due to the large dark current from bBP, it is hard to identify the photocurrent of the reference photodiode (PD) and the APD when we apply a light source at 3400 nm wavelength and 1 nW/μm^2 intensity to our device. Instead, we plot the responsivity of the reference PD, which is around 0.01 A/W, and the responsivity of the APD, which can reach as high as 2.75 A/W near the breakdown voltage, in Fig. 4(b).

Fig. 4(c) shows that a high small-signal-bandwidth up to 2.5 GHz can be obtained when APD operated at current gain equal to 10. The bandwidth is 1000 times larger than the other

known normal-incident 2DM-on-Si photodetectors to date [13-16], due to the thin 20 nm bBP thickness and the absence of photogating effect. In our simulation, we assume back side injection with uniform gold contact over the bBP so that a sufficiently high electric field can be applied across the heterojunction interface. The calculated GBP is 128.4 GHz when gain equals to 10.

The optimal noise-equivalent-power (NEP) of the device is ~70 pW/√Hz when the gain is around 20, as shown in Fig. 4(d).

IV. Conclusion

In this paper, we have concept-wise demonstrated MIR detector using bBP-on-Si heterostructure. The characteristics of bBP are discussed and modeled. Through avalanche multiplication, the proposed bBP-on-Si heterostructure APD responsivity can be up to theoretical maximum with high GBP of 128.4 GHz, which expands the possibility of high-speed MIR applications, such as optical communication and time-of-flight depth image sensing.

V. Reference

[1] A. Chaves et al., "Bandgap engineering of two-dimensional semiconductor materials," npj 2D Mater. Appl. **4**, 29 (2020).

[2] C. Liu et al., "Silicon/2D-material photodetectors: from near-infrared to mid-infrared," Light Sci. Appl. **10**, 123 (2021).

[3] Q. Guo et al., "Black Phosphorus Mid-Infrared Photodetectors with High Gain," Nano Lett. **16**, 4648 (2016).

[4] X. Chen et al., "Widely tunable black phosphorus mid-infrared photodetector," Nat. Commun. **8**, 1672 (2017).

[5] Y. Kang et al., "Monolithic germanium/silicon avalanche photodiodes with 340 GHz gain–bandwidth product," Nat. Photon. **3**, 59 (2009).

[6] Y. Akahama et al, "Electrical Properties of Black Phosphorus Single Crystals," J. Phys. Soc. Jpn. **52**, 2148 (1983).

[7] D. J. Perello et al., "High-performance n-type black phosphorus transistors with type control via thickness and contact-metal engineering," Nat Commun **6**, 7809 (2015).

[8] H. Asahina et al, "Band structure and optical properties of black phosphorus," J. Phys. C: Solid State Phys. **17**, 1839 (1984).

[9] S. M. Sze, "Physics of Semiconductor Devices", 2nd ed. Hoboken, NJ, USA: Wiley, (1985).

[10] S. M. Sze et al, "Avalanche breakdown voltages of abrupt and linearly graded p-n junctions in Ge, Si, GaAs and GaP," Appl. Phys. Lett. **8**, 111 (1966).

[11] R. J. McIntyre, "Multiplication noise in uniform avalanche diodes," IEEE Transactions on Electron Devices **13**, 164 (1966).

[12] R. B. Emmons, "Avalanche-photodiode frequency response," J. Appl. Phys. **38**, 3705 (1967).

[13] E. Wu et al., "In Situ Fabrication of 2D WS2/Si Type-II Heterojunction for Self-Powered Broadband Photodetector with Response up to Mid-Infrared," ACS Photonics **6**, 565 (2019).

[14] Nidhi et al., "Nanolayered Black Arsenic–Silicon Lateral Heterojunction Photodetector for Visible to Mid-Infrared Wavelengths," ACS Appl. Nano Mater. **3**, 9401 (2020).

[15] S. Luo et al., "High-performance mid-infrared photodetection based on Bi2Se3 maze and free-standing nanoplates," Nanotechnology **32**, 105705 (2021).

[16] M. Shawkat et al., "Scalable Van der Waals Two-Dimensional PtTe2 Layers Integrated onto Silicon for Efficient Near-to-Mid Infrared Photodetection," ACS Appl. Mater. Interfaces **13**, 15542 (2021).